AD-A037 502 ROCKWELL INTERNATIONAL THOUSAND OAKS CALIF SCIENCE --ETC F/G 20/12
SURFACE STUDY OF SEMICONDUCTOR DEVICES.(U)
MAR 77 R W GRANT N00014-75-C-0344
UNCLASSIFIED SC5016.7FR NL

1 OF 1
AD A037502

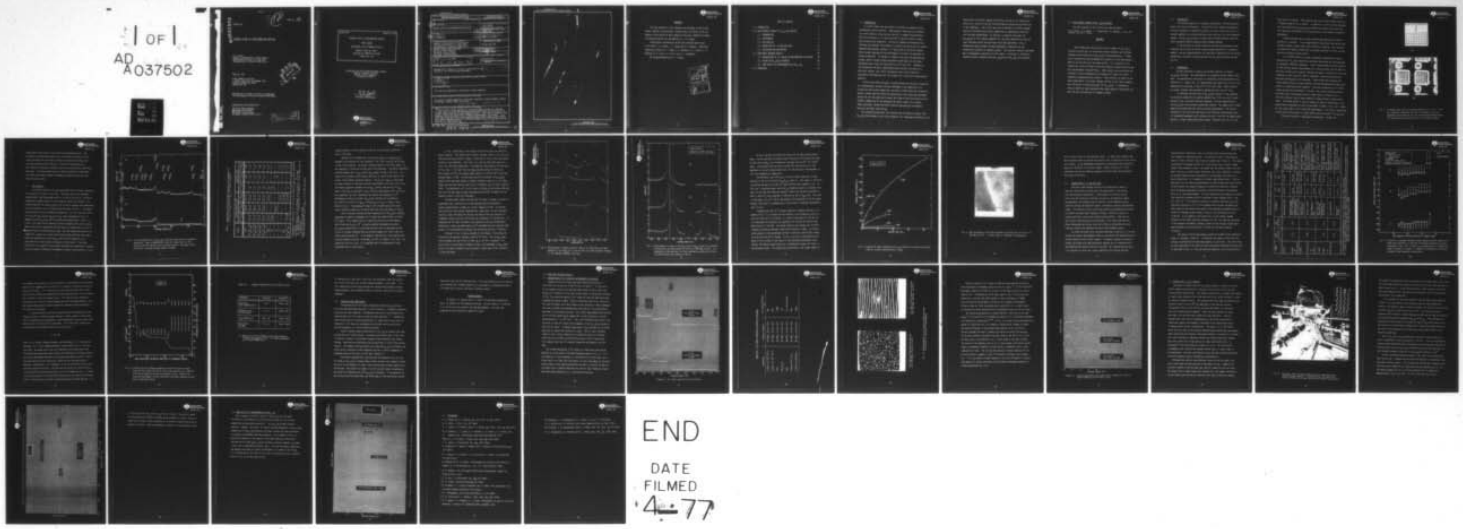

END

DATE FILMED
4-77

SURFACE STUDY OF SEMICONDUCTOR DEVICES

R. W. Grant
Rockwell International, Science Center
1049 Camino Dos Rios, P.O. Box 1085
Thousand Oaks, California 91360 U.S.A.

March 6, 1977

FINAL REPORT for Period
1 January 1975 thru 31 December 1976
Contract N00014-75-C-0344
Project No. 427

Sponsored by and prepared for

OFFICE OF NAVAL RESEARCH
Department of the Navy
800 North Quincy Street
Arlington, Virginia 22217 U.S.A.

SC5016.7FR March 6, 1977

SURFACE STUDY OF SEMICONDUCTOR DEVICES

FINAL REPORT

FOR PERIOD 1/1/75 THROUGH 12/31/76

General Order No. 5016
Contract No. N00014-75-C-0344
Project No. 427

Electronic and Solid State Sciences Program
Physical Sciences Division
Office of Naval Research
Arlington, VA 22217

R. W. Grant

R. W. Grant
Principal Investigator

Science Center
Rockwell International

1049 CAMINO DOS RIOS
THOUSAND OAKS, CALIF. 91360
805/498-4545

UNCLASSIFIED

SECURITY CLASSIFICATION OF THIS PAGE (When Data Entered)

REPORT DOCUMENTATION PAGE

READ INSTRUCTIONS BEFORE COMPLETING FORM

1. REPORT NUMBER	2. GOVT ACCESSION NO. / 3. RECIPIENT'S CATALOG NUMBER
4. TITLE (and Subtitle): SURFACE STUDY OF SEMICONDUCTOR DEVICES.	5. TYPE OF REPORT & PERIOD COVERED: Final Report 01/01/75 thru 12/31/76
	6. PERFORMING ORG. REPORT NUMBER: SC5016.7FR
7. AUTHOR(s): R. W. Grant	8. CONTRACT OR GRANT NUMBER(s): N00014-75-C-0344 new
9. PERFORMING ORGANIZATION NAME AND ADDRESS: Rockwell International, Science Center, 1049 Camino Dos Rios, P.O. Box 1085, Thousand Oaks, California 91360 U.S.A.	10. PROGRAM ELEMENT, PROJECT, TASK AREA & WORK UNIT NUMBERS: Project No. 427
11. CONTROLLING OFFICE NAME AND ADDRESS: Office of Naval Research, 800 North Quincy Street, Arlington, Virginia 22217	12. REPORT DATE: March 1977 / 13. NUMBER OF PAGES: 45
14. MONITORING AGENCY NAME & ADDRESS (if different from Controlling Office): Final rept. 1 Jan 75 - 31 Dec 76	15. SECURITY CLASS. (of this report): Unclassified / 15a. DECLASSIFICATION/DOWNGRADING SCHEDULE

16. DISTRIBUTION STATEMENT (of this Report)

Reproduction in whole or in part is permitted for any purpose of the United States Government.

DISTRIBUTION STATEMENT A
Approved for public release;
Distribution Unlimited

17. DISTRIBUTION STATEMENT (of the abstract entered in Block 20, if different from Report)

45 p.

18. SUPPLEMENTARY NOTES

This work was sponsored by the Office of Naval Research.

19. KEY WORDS (Continue on reverse side if necessary and identify by block number)

$Pb_{1-x}Sn_xTe$, surface chemistry, tellurides, ESCA/XPS, surface leakage current, Tellurium, surface oxides, $InAs_{1-x}Sb_x$

$Pb_{(1-x)}Sn_{(x)}Te$ $InAs_{(1-x)}Sb_{(x)}$

20. ABSTRACT (Continue on reverse side if necessary and identify by block number)

ESCA studies of $Pb_{1-x}Sn_xTe$ and a few $InAs_{1-x}Sb_x$ surfaces are reported. A diode array structure has been developed to facilitate the correlation of surface composition and surface leakage currents. ESCA results establish that elemental tellurium layers form on several semiconductor tellurides. It is shown that these tellurium layers on $Pb_{1-x}Sn_xTe$ diodes produce exceptionally low surface leakage currents at 77°K which suggests that Te° may be a surface passivant for $Pb_{1-x}Sn_xTe$.

elemental Te

DD FORM 1 JAN 73 1473 EDITION OF 1 NOV 65 IS OBSOLETE

389 949

UNCLASSIFIED

SECURITY CLASSIFICATION OF THIS PAGE (When Data Entered)

LB

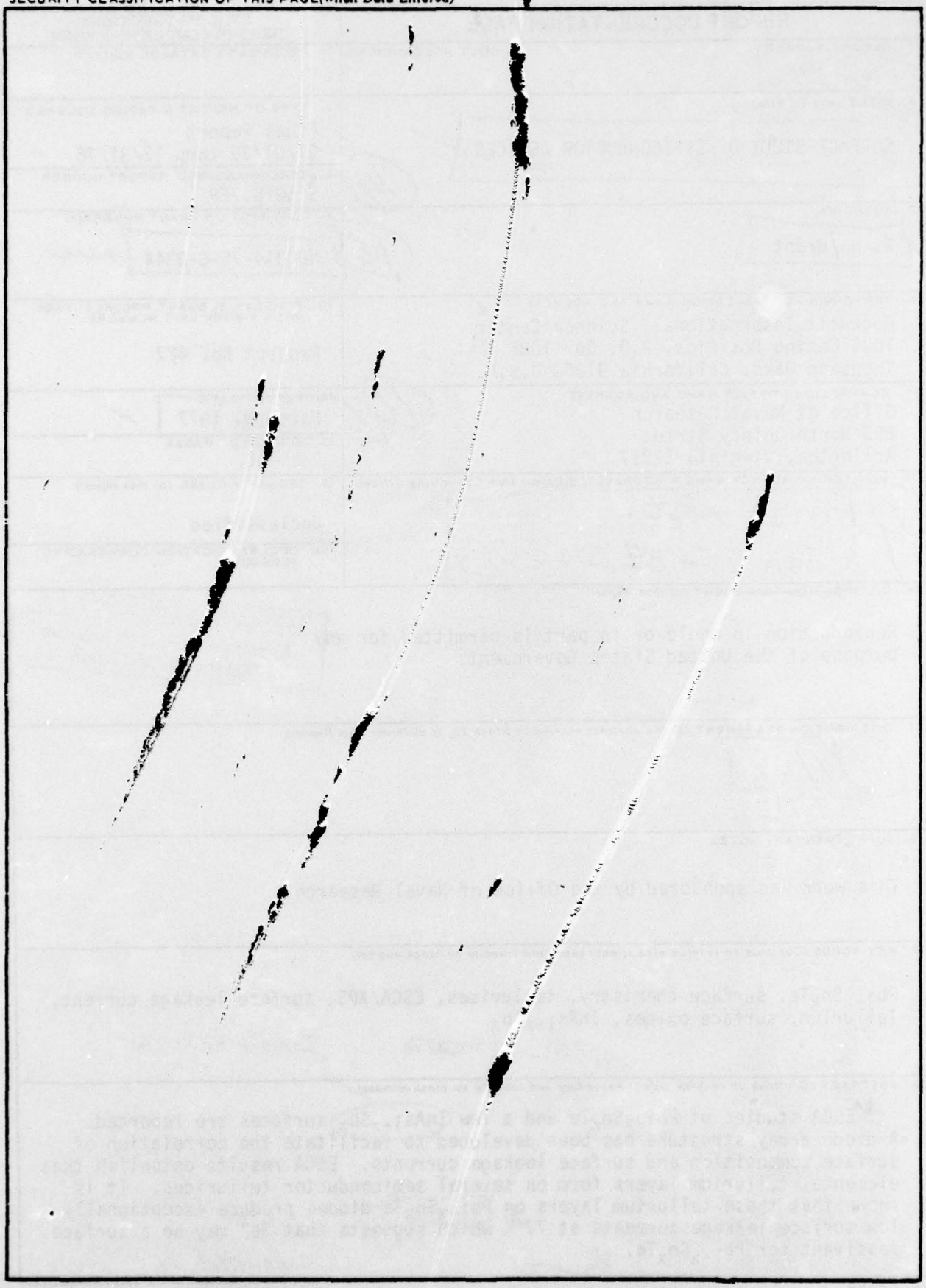

FOREWARD

The work reported in this document was performed at the Science Center, Rockwell International, Thousand Oaks, California, with the support of the Office of Naval Research (Contract # N00014-75-C-0344). The contract monitor for the ONR was Dr. L. R. Cooper.

Investigators contributing to the work reported herein were R. W. Grant, J. G. Pasko, J. T. Longo and A. M. Andrews. Additional support was given by P. C. Wang, E. R. Gertner, J. E. Clarke, J. R. Waldrop, M. D. Lind, E. H. Cirlin and F. J. Szalkowski.

The program manager was A. S. Joseph.

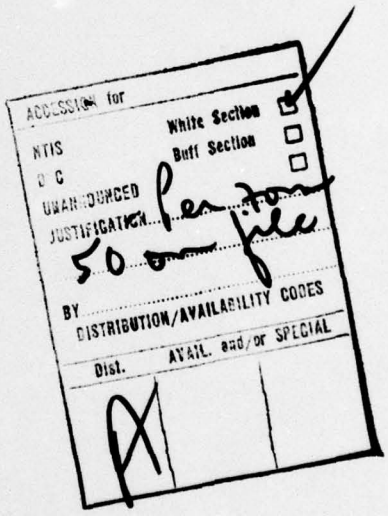

TABLE OF CONTENTS

1.0 INTRODUCTION

It is well known that the nature of surfaces can markedly affect semiconductor device behavior. Semiconductor technology has advanced to a point where by using the wide variety of compound semiconductors which are available, it is often possible to design a device to meet desired electrical properties. The use of compound semiconductors has increased considerably the problem of surface passivation and for several compound semiconductor systems it is found that the deviation between device design expectations and performance is directly attributable to surface properties. At present, it appears that most new semiconductor systems require unique surface passivation techniques and that these techniques must largely be discovered by trial and error. Compared to the information and basic understanding which permits the design of a particular device, very little information exists which predicts a passivation technique that will be suitable for a particular semiconductor material.

A first step toward the goal of understanding the electronic properties of a semiconductor surface involves knowledge of the composition of a surface and how surface composition variations affect electrical properties. Several surface sensitive electron spectroscopic tools have been developed during the last few years which permit the study of both the electrical and chemical composition of the outermost few atomic layers of a surface. These techniques include both ESCA (electron spectroscopy for chemical analysis) and Auger spectroscopy.

The program pursued under this contract was initiated in January 1975. $Pb_{1-x}Sn_xTe$ was chosen as the initial material for investigation because of its

long history of surface leakage difficulties and due to its ready availability as a result of the far-infrared imaging program being carried out in our laboratory. The initial goal was to determine if surface leakage could be correlated with surface composition as determined by ESCA and this has been accomplished. In addition, a potential passivant for $Pb_{1-x}Sn_xTe$ at 77°K, namely elemental Te°, has been identified and the Te° layer thickness useful for passivation has been determined. Also, a dimensional analysis model has been developed to separate bulk and surface contributions to leakage currents. This work was recently published and is reproduced in Section 2 of this report. In Section 3, additional research results related to both $Pb_{1-x}Sn_xTe$ and $InAs_{1-x}Sb_x$ are presented.

2.0 ESCA SURFACE STUDIES OF $Pb_{1-x}Sn_xTe$ DEVICES

The work reported in this section has been published:

R. W. Grant, J. G. Pasko, J. T. Longo and A. M. Andrews, *J. Vac. Sci. Technol.* 13, 940-7 (1976).

ABSTRACT

ESCA studies have been carried out on a number of $Pb_{1-x}Sn_xTe$ surfaces with the goal of correlating surface chemistry with surface leakage currents observed in $Pb_{1-x}Sn_xTe$ infrared detectors. A diode array structure has been developed which permits I-V and ESCA measurements to be carried out on the same surface. It is possible to reprocess this array to change the surface chemistry without altering the bulk semiconductor characteristics. ESCA results have established the existence of thick (hundreds of Å) elemental Te^0 layers on several chemically processed device surfaces. These surfaces are shown to produce exceptionally low surface leakage currents at 77°K which suggests that Te^0 may be a surface passivant for $Pb_{1-x}Sn_xTe$. A dimensional analysis model has been developed which seems capable of estimating surface and bulk contributions to leakage currents.

2.1 INTRODUCTION

The surface properties of compound semiconductor infrared detectors often limit device performance. The passivation of compound semiconductor surfaces represents a substantial problem, at least in part due to the increased complexity of surface chemistry which can occur in a multicomponent system. The $Pb_{1-x}Sn_xTe$ system is among those infrared detector materials which frequently exhibit marked surface leakage problems.

If correlations of surface chemistry and device performance can be obtained, one can hope to reduce surface leakage problems by a systematic method. The work reported herein will describe an approach which we believe establishes a potential surface passivant for $Pb_{1-x}Sn_xTe$ devices operated at 77° K.

2.2 EXPERIMENTAL

We have used ESCA to examine the surface chemistry of several $Pb_{1-x}Sn_xTe$ surfaces. Our spectrometer is the Hewlett-Packard 5950A instrument. The photoelectric excitation is achieved by using monochromatic AlK_α radiation ($h\nu$ = 1486.6 eV). All measurements were made within 15° C of room temperature at pressures in the 10^{-8} to 10^{-9} torr range. Depth profiles of several surfaces were obtained by sputtering with 1 keV Ar^+ ions.

To interpret the ESCA data on $Pb_{1-x}Sn_xTe$ surfaces it was necessary to accurately determine the binding energies (E_B) of Pb, Sn, and Te photoelectron lines in several reference compounds. Various compositions of the $Pb_{1-x}Sn_xTe$ solid solution system were studied. The composition of these samples was determined from lattice constant measurements. The lattice constants of PbTe and SnTe were found to be 6.462 and 6.318Å respectively (in reasonable agreement with literature values)[1,2] and for the compositional analysis a linear interpolation was assumed. Samples of Pb, Sn, Te, and

TeO_2 were also studied. These samples were from various sources and were of reagent grade purity or better. In addition, a solid solution specimen with the composition $Pb_{.04}Te_{.96}$ was prepared by quenching from the melt; this sample was determined to be single phase by X-ray powder diffraction photography.

Sample charging can be a major problem when determining binding energies of insulators. It was experimentally determined that none of the reference samples (except TeO_2) were affected by charging. This was done by flooding the sample surface with low energy electrons (0-10 eV) and observing the absence of peak shifts.

It is often difficult to obtain completely reproducible surface properties on $Pb_{1-x}Sn_xTe$ materials even when these materials are processed by supposedly identical procedures. Thus it was decided to perform electrical and surface chemical measurements on a single surface with the hope of partially avoiding this problem. Because the spatial resolution of the ESCA technique is poor (typically $1mm^2$ is analyzed), large area diode arrays have been fabricated for this purpose. These arrays were produced from liquid phase epitaxially grown material[3] and the heterojunction diodes were similar to those previously reported.[4] The array dimensions are $\approx$ 0.76cm x 0.76cm and the layer thickness is $\approx$ 0.5mm. Two slightly different arrays have been used; a photograph of one of these arrays is shown in Fig. 1. The array contains rows of equal numbers of large and small diodes (63 of each). The diodes differ in area by roughly an order of magnitude; a high magnification photograph of some of the diodes is shown in Fig. 1(b). There are two large areas to facilitate ESCA measurements. The array is fabricated so that one of these areas is a PbTe surface while the other is $Pb_{.8}Sn_{.2}Te$.

The entire surface is processed simultaneously. Diodes are

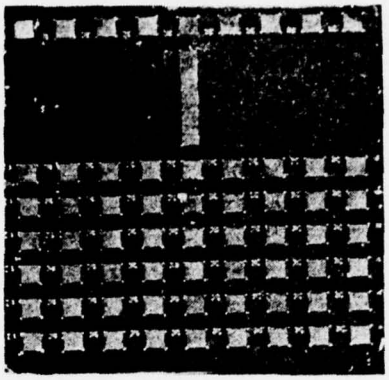

(a)

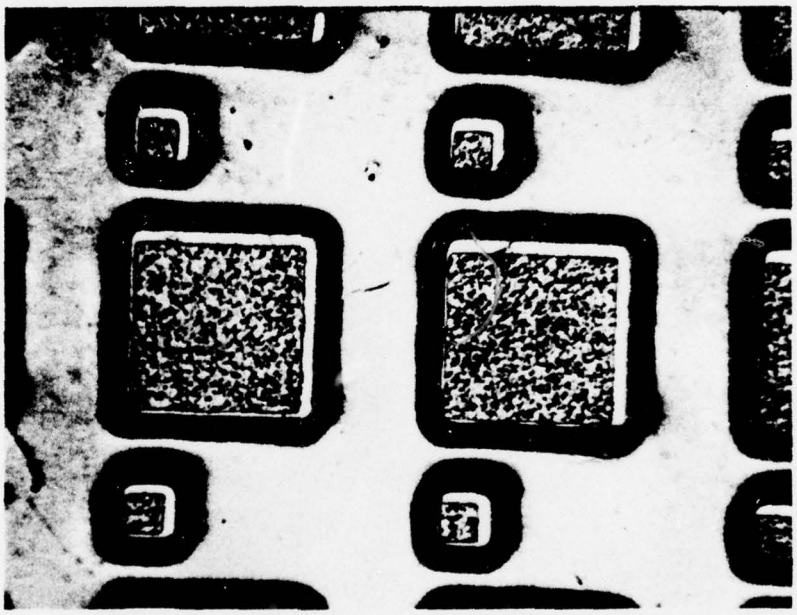

(b)

Fig. 1 (a) Diode array used to correlate ESCA and I-V (≈ 7 X). The two large dark areas near the top of the photo, which are separated by the vertical bar, are the ESCA measurement areas; (b) high magnification photo (64 X) of individual diodes.

positioned on both sides of the large ESCA measurement areas. The uniformity of diode characteristics as a function of position in the array indicated that the diode surfaces and large-area surfaces had the same average surface chemistry. Electrical measurements are facilitated by probing Au contacts which are electroplated on the diode mesa tops. The entire diode array can then be chemically reprocessed to change the surface chemistry presumably without altering the bulk device characteristics.

2.3 ESCA RESULTS

A 0-1000 eV scan of a $Pb_{.62}Sn_{.38}Te$ sample which had been cleaned by Ar^+ sputtering is shown in Fig. 2(a). The most intense and narrowest photoelectron lines associated with Pb, Sn, and Te are the 4f, 3d and 3d respectively (these levels all have large spin-orbit splittings). The binding energies for the $Pb_{1-x}Sn_xTe$, Pb, Sn and Te samples were determined with an accuracy of ±0.1 eV; these data are given in Table I. The sample surfaces were initially cleaned by sputtering. The line intensity ratios ($Pb\ 4f_{7/2}/Te\ 3d_{5/2}$ and $Sn\ 3d_{5/2}/Te\ 3d_{5/2}$) were determined for the six members of the $Pb_{1-x}Sn_xTe$ solid solution system mentioned in Table I. To within ≈ 10% these ratios remained constant throughout the entire system. After subtracting a background function which was proportional to the integrated area of the photoelectron peak, the line shapes were found to be symmetrical (except for a small high binding energy shoulder which sometimes was detectable on the $Sn\ 3d_{5/2}$ line and which appeared to be associated with a small amount of oxygen on the surface). The above analysis of line intensities and shapes indicated that preferential sputtering, which might be expected from momentum transfer considerations, is not

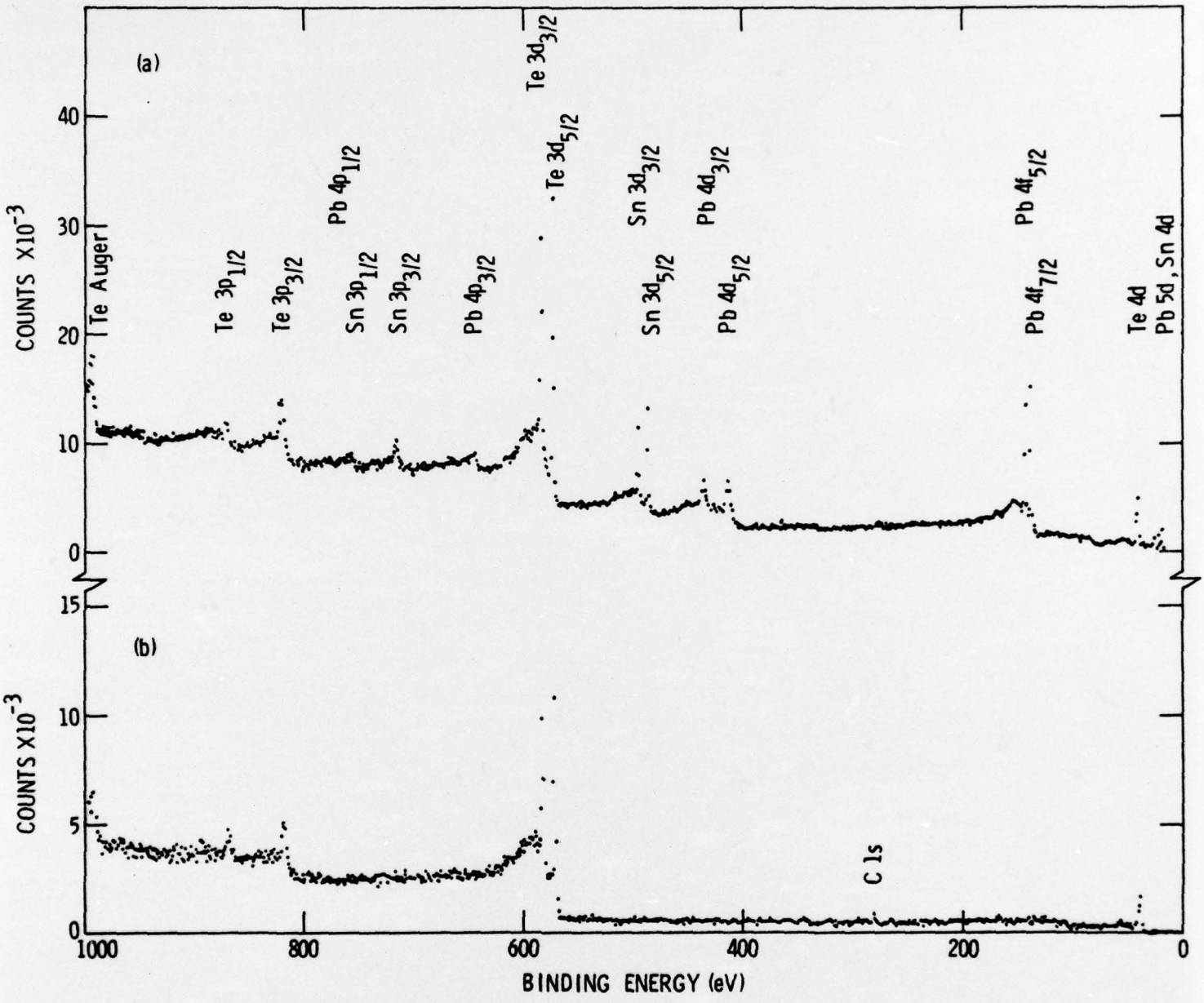

Fig. 2 (a) ESCA spectrum of $Pb_{.62}Sn_{.38}Te$ specimen which had been cleaned by sputtering. Major photoelectron lines are identified; (b) ESCA spectrum of PbTe specimen which had been etched in 20% HNO_3 for 98 min at 24°C (surface was <u>not</u> sputter cleaned).

TABLE I. Experimentally Measured Binding Energies and Linewidths of Pb $4f_{7/2}$, Sn $3d_{5/2}$ and Te $3d_{5/2}$ for Several Samples[a]

Sample	Binding Energy (eV)[b]			Linewidth (eV)[c]		
	Pb $4f_{7/2}$	Sn $3d_{5/2}$	Te $3d_{5/2}$	Pb $4f_{7/2}$	Sn $3d_{5/2}$	Te $3d_{5/2}$
SnTe	--	485.37	572.32	--	1.09	1.09
$Pb_{.18}Sn_{.82}Te$	137.32	485.46	572.34	.84	1.21	1.14
$Pb_{.42}Sn_{.58}Te$	137.25	485.52	572.19	.75	1.16	1.07
$Pb_{.62}Sn_{.38}Te$	137.34	485.53	572.12	.83	1.05	1.09
$Pb_{.81}Sn_{.19}Te$	137.43	485.66	572.26	.85	1.17	1.09
PbTe	137.43	--	572.19	.81	--	1.01
Pb	136.93	--	--	.84	--	--
Sn	--	484.76	--	--	.95	--
Te	--	--	573.04	--	--	1.10
TeO_2	--	--	576.39[d]	--	--	1.41
$Pb_{.04}Te_{.96}$	137.39[d]	--	573.04[d]	.91	--	1.17

[a] Uncertainty in most values is ≈ ±0.1 eV; for TeO_2 & $Pb_{.04}Te_{.96}$ data, uncertainty is ±0.2 eV.

[b] All binding energies (E_B) are referenced to E_B of Au $4f_{7/2}$ in Au metal (E_B = 84.00 ± 0.01eV) as measured by F. R. McFeely, et al., Phys. Rev. 7B, 5228 (1973).

[c] Full width at half peak height.

[d] Data are normalized to E_B of Te $3d_{5/2}$ in Te or PbTe (see text).

a major problem in the $Pb_{1-x}Sn_xTe$ system for the sputtering conditions used in this work.

Because of its composition, the E_B of Te $3d_{5/2}$ in $Pb_{.04}Te_{.96}$ was assumed to be identical to that observed in Te^o; this fixed E_B for Pb $4f_{7/2}$ in this solid solution. To control charging effects in the TeO_2 sample, it was necessary to flood the surface with 10 eV electrons. The energy separation observed between the O $1s_{1/2}$ and Te $3d_{5/2}$ peaks in TeO_2 is 45.70 eV. Surfaces of Te and PbTe, which contain very thin (a few Å) oxide layers of Te oxide, do not exhibit charging problems. The E_B of Te $3d_{5/2}$ in the oxide on these surfaces is the same to within experimental error (±0.1 eV); also, the energy separation between the Te $3d_{5/2}$ (oxide) peak and the O $1s_{1/2}$ peak is the same as observed in TeO_2 to within experimental error (±0.2 eV). We, therefore, use this information to identify the presence of Te^{4+} (presumably as TeO_2) on several $Pb_{1-x}Sn_xTe$ surfaces and to establish E_B = 576.39 ±.2 eV for Te $3d_{5/2}$ in TeO_2; E_B of O $1s_{1/2}$ in TeO_2 is thus 530.69 ±0.2 eV. The presence of TeO_2 on Te^o surfaces agrees with macroscopic oxidation studies of Te^o which show that the oxide phase is TeO_2.[5]

One of the most interesting ESCA observations on $Pb_{1-x}Sn_xTe$ surfaces subjected to chemical treatments has involved the identification of thick Te^o layers. This identification is made from the value of the chemical shift (note that E_B for Te^{2-} is nearly constant throughout the entire $Pb_{1-x}Sn_xTe$ system (Table I)), and from the fact that in some cases Pb and Sn are so strongly depleted that the surface composition itself rules out almost everything but Te^o. As an example, ESCA data on a PbTe sample which had been etched for 98 min in 20% HNO_3 (at 24°C) is shown in Fig. 2(b). By comparison with Fig. 2(a), it is observed that all photoelectron lines associated with Pb are missing.

In Fig. 3 ESCA data in the region of the Te 3d lines are shown for several samples. The sample used to obtain the data shown in Fig. 3(a) was PbTe which had been etched in H_2SO_4. Three sets of Te 3d lines are clearly visible in this spectrum. Figs. 3(b), (c), and (d) show ESCA spectra of PbTe, Te^0, and TeO_2 respectively. By comparing these spectra with the data of Fig. 3(a), it is clear that the H_2SO_4 treated surface of PbTe has a small amount of Te^{4+}, and roughly equal amounts of Te^0 and Te^{2-} within the analyzed depth ($\approx$ 15Å). We have observed Te^0 on surfaces of $Pb_{1-x}Sn_xTe$ samples which have been etched in several different acids (e.g., HF, HNO_3, H_2SO_4, and the Coker HBr-Br_2 etch[6] which is commonly used in device fabrication). The observation of a Te-rich layer on $Pb_{.8}Sn_{.2}Te$ following a HBr-Br_2 etch has also been made by Auger spectroscopy but direct evidence for the chemical state of Te was not obtained.[7]

To obtain some insight into how the Te^0 layer is formed, a series of experiments was carried out on a PbTe specimen which was etched in several concentrations of HNO_3 for various lengths of time. To minimize the possibility that crystal imperfections, impurities, carrier concentration etc. might influence the results, the same crystal was used for all treatments (after each etch the surface was cleaned by Ar^+ sputtering). To determine the Te^0 layer thickness, the sputtering rate was calibrated by sputtering a highly polished sample of Te^0 and measuring the resulting step height in an interference microscope (the sputtering rate was $\approx$ 21Å/min).

The data in Fig. 4 show an example of the change in line shape and position as one sputters through a typical Te^0 layer. The Te $3d_{5/2}$ peak first broadens and then shifts to lower E_B as the Te^0 is removed. On a fairly thick (on the order of 1000Å) Te layer, the broadened Te $3d_{5/2}$ peak exists for several hundred Å which provides a rough idea of the uniformity in layer thickness.

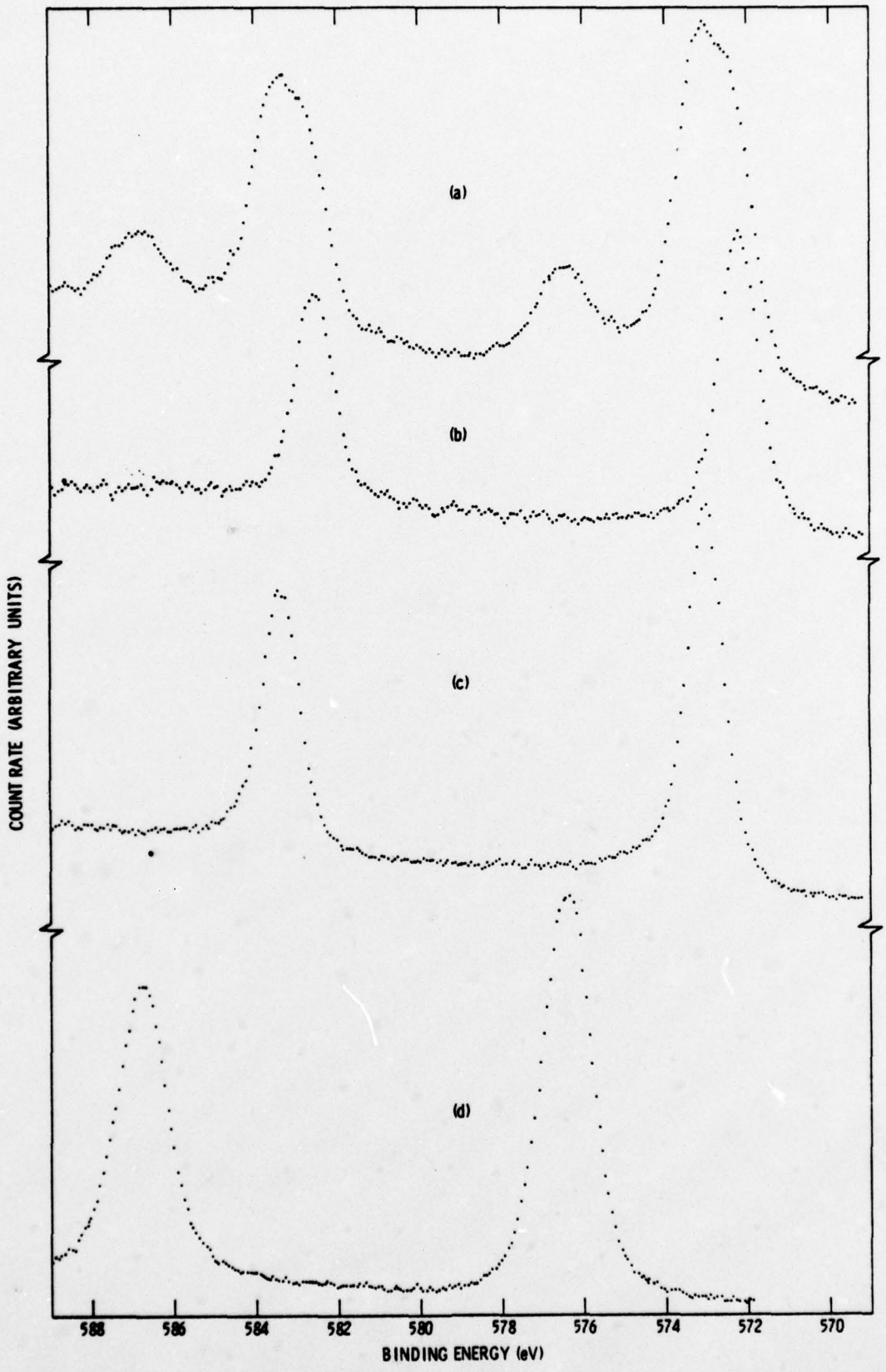

Fig. 3 ESCA spectra in region of Te 3d lines of (a) PbTe which had been etched in ≈ 17% H_2SO_4 for 10 min at 35°C, (b) PbTe (sputter cleaned), (c) Te (sputter cleaned), (d) TeO_2.

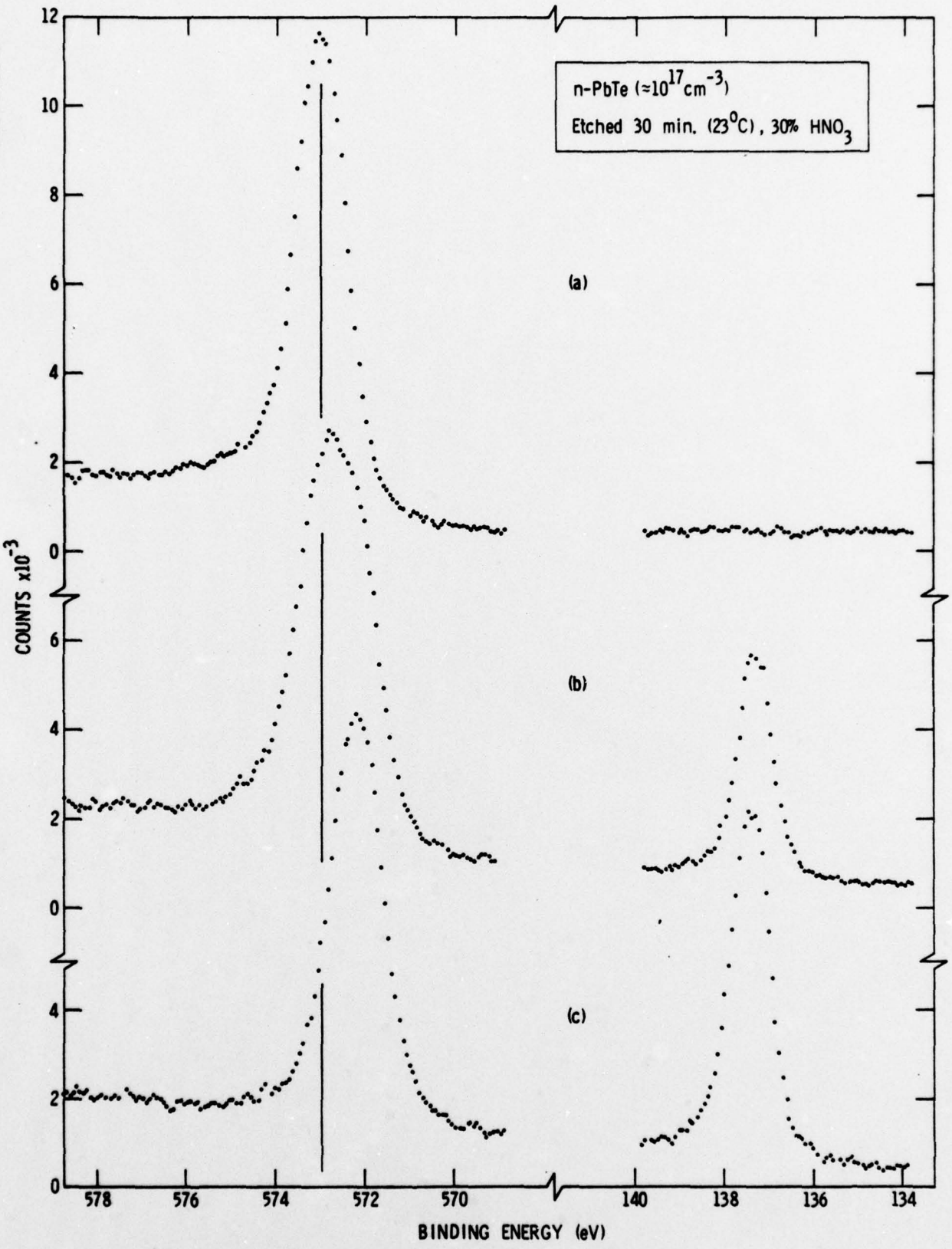

Fig. 4 ESCA spectra in region of Pb $4f_{7/2}$ and Te $3d_{5/2}$ lines for a specimen of PbTe which had been etched for 30 min in 30% HNO_3 at 23°C. (a) immediately after etching, (b) after sputtering surface for 30 min, (c) after sputtering surface for 46 min.

In Fig. 5 we have collected the results of our HNO_3 etching experiments. We have defined the average layer thickness as the sputtering depth at which the Te $3d_{5/2}$ line intensities from both Te^0 and Te^{2-} are roughly equal. One observes that the rate at which the layer builds up is very dependent on the acid concentration and, for the one point investigated, is also very dependent on temperature.

Unfortunately, E_B of Pb $4f_{7/2}$ in PbTe is almost identical to that observed in the solid solution $Pb_{.04}Te_{.96}$ (Table I). This makes it difficult to conclude whether or not the Te^0 layer contains small amounts of Pb. As the layer is sputtered away, the Pb $4f_{7/2}$ intensity begins to increase; however, by the time the intensity reaches $\approx$ 15% of the intensity observed in PbTe, a definite low E_B shoulder is observed on the Te $3d_{5/2}$ line. This sets a crude upper limit of $\approx$ 15% on the amount of Pb contained in the Te^0 layer; however, the actual Pb concentration in this layer is probably considerably less (if any).

Assuming that the Te^0 is being formed by a chemical reaction, as it appears to be, it is curious why the reaction is not stopped as soon as a very thin layer of Te is formed, i.e., what is the source of the new Te? To investigate this question, we examined a Te^0 surface on PbTe at high magnification in the SEM. The sample used for this purpose was initially cleaned by sputtering through a mask before etching in HNO_3. The native oxide present on the unsputtered surface is found to significantly reduce the rate at which Te^0 is formed. In Fig. 6 we show a high magnification photo of this surface in the region of the sputtered/unsputtered intersection (the darker region which has a considerably thicker Te^0 layer is the sputtered area). The interesting observation is the larger number of

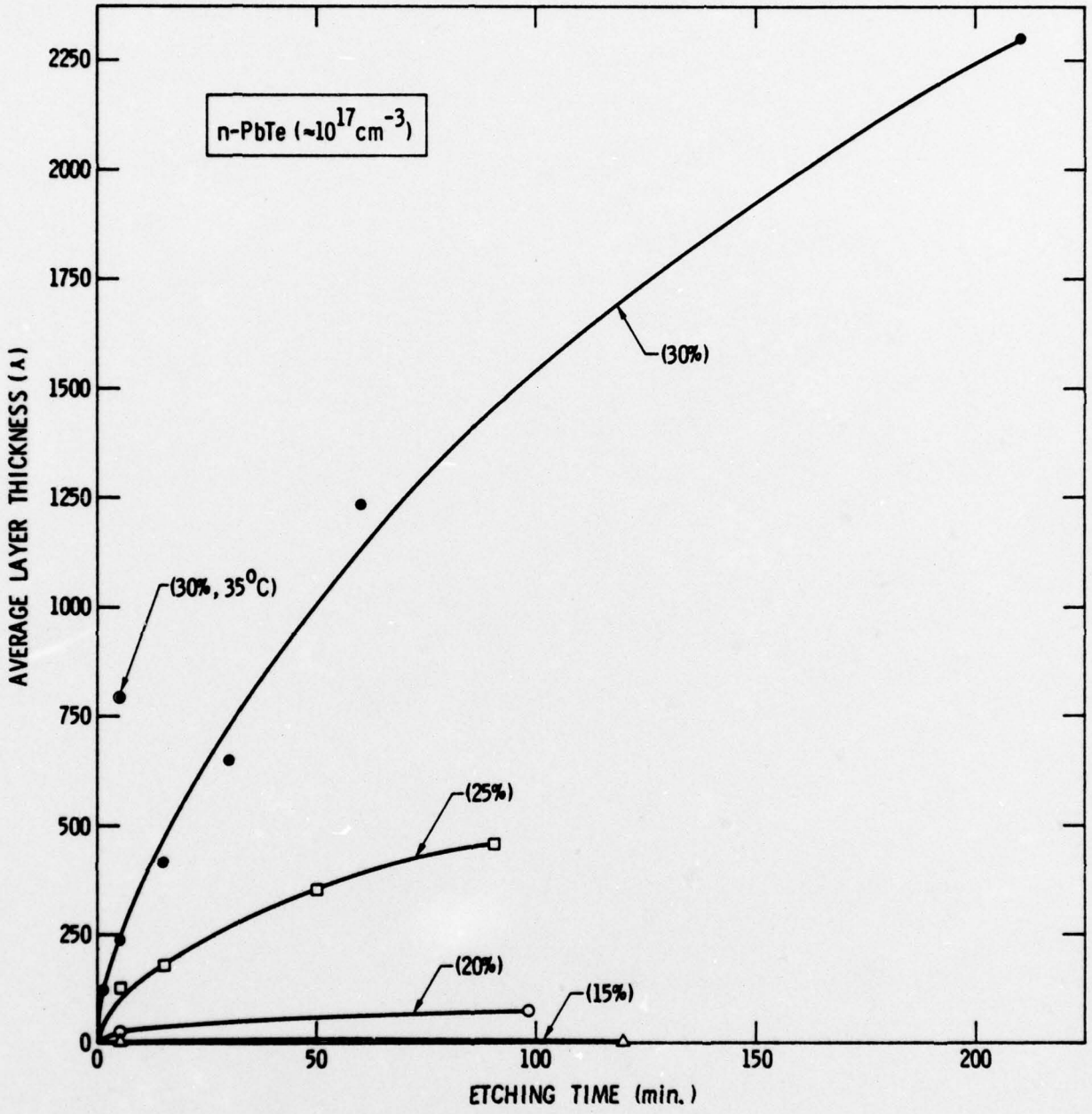

Fig. 5 Average Te^0 layer thickness built up on PbTe as a function of etching time for various concentrations of HNO_3.

Fig. 6 SEM micrograph of Te^{o} layer produced by etching PbTe for 20 min in 25% HNO_3 at 23°C. 1 micron scale is indicated in photograph.

pits on the Te layer in the sputtered region. If these pits extend to the PbTe substrate they may provide the source of new Te required to build up the thick layers. In an independent measurement we determined the dislocation density ($\approx 2 \times 10^7 cm^2$) in this PbTe sample. Within a factor of ≈ 3 this correlates with the pit density observed on the Te^0 layer and may explain the origin of the pits.

2.4 CORRELATION OF I-V AND ESCA DATA

The total diode leakage current can be described in terms of both bulk and surface currents which are proportional to the device area and perimeter respectively. Contributions to the bulk current arise from the diffusion of minority carriers to the depletion region, the generation and recombination of carriers in the depletion region, tunneling through the depletion region, and defects shunting the depletion region. The surface currents arise from generation-recombination currents at surface inversion and/or depletion regions, tunneling currents at surface junctions, and current through surface defects. When the surface current contribution can be minimized, it has been observed[8] that PbSnTe heterojunction devices have bulk diffusion and generation-recombination currents that dominate the total diode leakage current.

By using the diode array structure described in Section 2.2, we have carried out several measurements aimed at correlating ESCA determinations of surface chemistry with surface leakage. The general approach has been to process the diode array described above, measure the I-V characteristics and determine the surface chemistry with ESCA. By reprocessing the array, it is possible to alter the surface chemistry while leaving the bulk

characteristics unaffected. Both I-V and ESCA data were obtained after each sequential reprocessing step. The results of some of these measurements on three different diode arrays are summarized in Table II. The number distribution of leakage currents of a given diode size is usually skewed toward large leakage currents. We assume that the poorest diodes have some major flaw (e.g., cracks, metal inclusions, etc.) and, therefore, to obtain an average leakage current characteristic of the defect-free parts of a given diode array, it is necessary to reject these observations. This has been done first by rejecting measurements on those diodes which have obvious visible defects and second by applying a statistical rejection criterion which eliminates measurements outside a certain multiple of the probable error for a single measurement. For this purpose we have adapted the typical data rejection procedure which is described in many standard texts (see e.g., Ref. 9). This rejection criterion is obviously arbitrary; we find that data rejection at $\approx 2.5 \rightarrow 4.0$ probable errors brings the median and mean values of the current distribution into reasonable agreement and the values for leakage currents shown in Table II are consistent with this criterion. As an example of the sensitivity of the average leakage currents to this data rejection procedure, in Fig. 7 we show the variation in the average (and median) leakage currents of the 50 small diodes which were analyzed on array #6-313A as a function of the data rejection criterion.

The effect on the diode leakage currents of several array processing steps is indicated in Table II. In addition, the nature of the Te on the surface as determined from ESCA measurements is also given. The "acid clean-up etch" mentioned in the table has been discussed by Andrews;[10] the Norr etch is described in Ref. 11. From the table one observes a very strong correla-

TABLE II. Variation of Diode Leakage Currents for 3 Arrays which had several sequential surface treatments

ARRAY	LDA[a] ($10^{-3}cm^2$)	SDA[a] ($10^{-4}cm^2$)	TREATMENT	$\bar{L}_L$[b] (ma)	$\bar{L}_S$[b] (ma)	NATURE OF SURFACE Te AS DETERMINED BY ESCA
6-313A	1.75	1.59	$HBr-Br_2$ mesa etch	.65±.012	.17±.015	Surface completely oxidized (Te^{4+}). Sputtering indicated some Te^0 in layer ≈ 40Å thick
n-PbTe on $p-Pb_{.8}Sn_{.2}Te$			Sputter cleaned; 24 hr. air exposure	.74±.06	.275±.015	Several monolayers of oxide (Te^{4+}). No Te^0
			Sputter cleaned; acid clean-up etch	.030±.010	.0077±.0006	Small amount superficial Te^{4+}; Te^0 layer ≈ 200Å thick
5-270A	1.49	1.13	Norr etch; acid clean-up etch	.130±.025	.0145±.0015	Several monolayers of Te^{4+}; Te^0 layer ≈ 300Å thick
$p-Pb_{.8}Sn_{.2}Te$ on n-PbTe			Sputter cleaned	5.4±.9	1.25±.2	Only Te^{2-} (except for small amount of native oxide formed during few hours air exposure)
			Acid clean-up etch	.21±.02	.0205±.0015	Several monolayers Te^{4+}; Te^0 layer ≈ 130Å thick
2-132C	1.52	1.11	Norr etch; acid clean-up etch	2.53±.15	.174±.015	Thick Te^0 layer, small amount of Te^{4+}
n-PbTe on $p-Pb_{.8}Sn_{.2}Te$			Exposed to air for few hours	2.8±.4	.175±.025	Thick Te^0 layer, oxide layer ≈ 3 times thicker than after Norr etch
	1.30	0.62	H_2O_2 based etch	14± 1.25	2.5±.3	Small amount of Te^0; bulk Te^{2-} observable, several monolayers of oxide
			Norr etch; 9% HNO_3	8.2±1.4	1.05±.2	Small amount of Te^0; bulk Te^{2-} observable, small amount surface oxide

a) LDA and SDA are average geometrical areas of large and small diodes respectively.
b) $\bar{L}_L$ and $\bar{L}_S$ are average 77° K leakage currents observed at small reverse bias based on 2.5→4.0 probable error data rejection criterion as described in text. Leakage currents for array 6-313A were measured at -100mV; for the other 2 arrays, they were measured at -250mV.

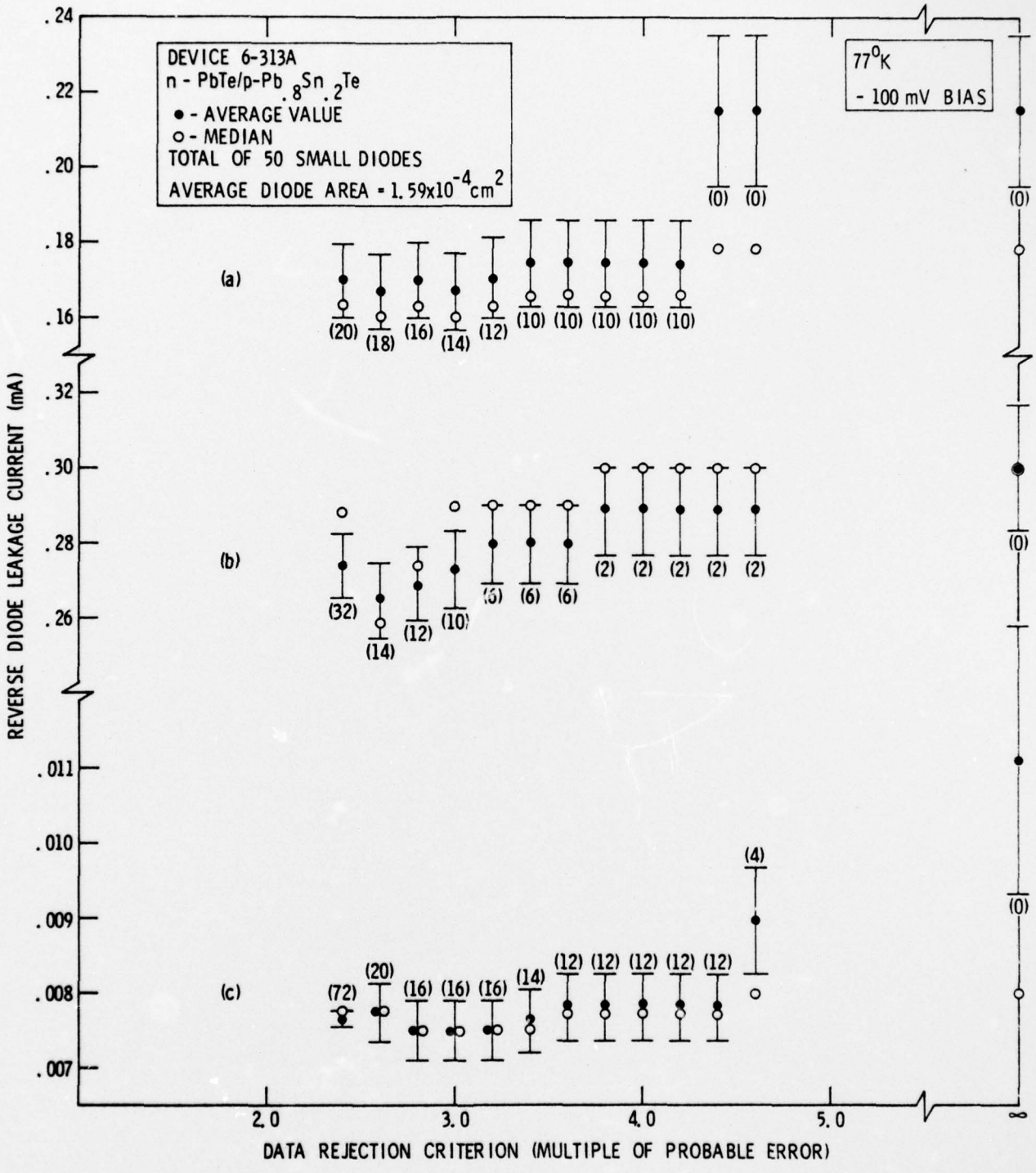

Fig. 7 Variation in average and median diode leakage currents observed for diode array #6-313A as a function of the data rejection criterion discussed in text. (a), (b) and (c) correspond to the 3 processing steps referred to in Table II. Numbers in parenthesis are the percentage of data rejected at each point.

tion between the presence of thick Te^0 layers on the surface and low leakage devices which suggests that at 77° K, Te^0 is a potential surface passivant for $Pb_{1-x}Sn_xTe$ devices. It is interesting to note from the table that in the case of array #5-270A, low leakage devices were obtained after initial processing to obtain a thick Te^0 surface layer. This layer was then removed by sputtering with 1 keV Ar^+ and the leakage currents increased markedly. The low leakage characteristics were essentially restored by again applying a Te^0 layer to the surface.

It would be useful to extract surface and bulk contributions to the leakage currents in order to assess how well a given surface is passivated. For this purpose we have developed a simple dimensional analysis model which seems capable of providing this separation. At a fixed small reverse bias we assume that the leakage current can be expressed as

$$i = SP + BA$$

where S is a surface leakage parameter (current/length), P is the junction perimeter, B is a bulk leakage parameter (current/area) and A is the junction area. We assume that P and A are defined by the etched mesa sizes. The diode arrays described herein contain two different size diodes; thus we solve two simultaneous equations of the type shown above to obtain S and B. The same statistical data rejection criteria as was discussed above is applied in the analysis. As an example, in Fig. 8 we show how S and B vary with data rejection criteria. We note that the values of S and B are not overly sensitive to data rejection at $\approx 2.5 \rightarrow 4.0$ probable errors. In Table III we give values of S and B derived from data for the diode array #2-132C (which is the only case in which a detailed analysis has been applied). It

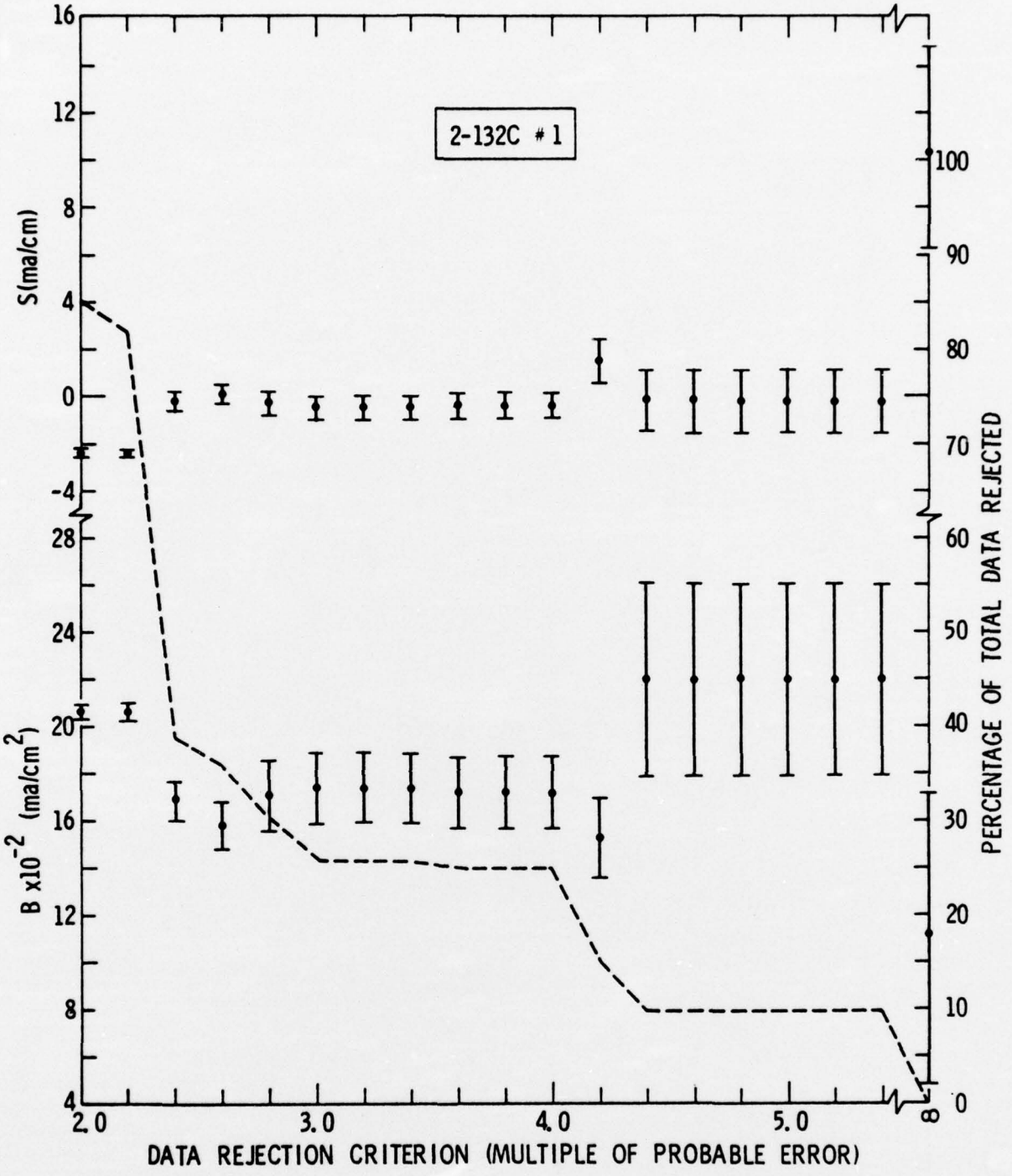

Fig. 8 Surface and bulk leakage parameters derived from data on diode array #2-132C (after the initial acid clean-up etch) as a function of the data rejection criteria discussed in text. Dashed line shows the percentage of total data which have been rejected at each point (right-hand scale).

TABLE III. LEAKAGE CHARACTERISTICS FOR ARRAY #2-132C

TREATMENT	S(ma/cm)[a]	B(ma/cm^2)[a]
Norr etch; acid clean-up etch	0 ± 1	1750 ± 200
Exposed to air for few hours	-1 ± 1	1850 ± 350
H_2O_2 based etch	80 ± 15	2300 ± 1300
Norr etch; 9% HNO_3	27 ± 8	2700 ± 1300

a) Based on 2.5→4.0 probable error data rejection criterion described in text. S & B were evaluated at 77° K and -250mV bias.

is interesting to note that in the first two treatments where the surface has a thick Te^0 layer, the surface leakage parameter is very small. It is also interesting to note that although the average diode leakage currents change markedly, the B parameter remains relatively insensitive to surface treatment.

2.5 DISCUSSION AND CONCLUSIONS

The observation of Te^0 layers produced by etching $Pb_{1-x}Sn_xTe$ with acids has been mentioned previously in the literature,[12] although no detailed discussion has been reported. Considerably more work on the formation and characterization of Te^0 layers on CdTe has been reported.[12-15] Considering these results and our current observations, it seems quite likely that the formation of Te^0 layers on semiconductor tellurides during certain acid etching procedures is a fairly common occurrance.

Several studies aimed at passivation of $Pb_{1-x}Sn_xTe$ surfaces have been carried out with limited success. We believe the current work is the first to identify a specific relationship between surface chemistry and surface leakage. Some previous observations may be explained in view of the current results. For example, the observation that treating $Pb_{1-x}Sn_xTe$ surfaces with mildly acidic solutions of EDTA sometimes resulted in device impedance improvement might be the result of Te^0 layer formation.[16]

The results reported here indicate that the presence of Pb, Sn, and Te oxides on $Pb_{1-x}Sn_xTe$ surfaces almost always produces high leakage currents. The role of the elemental Te layer in passivating these surfaces needs to be established. One possibility seems to be that surface states introduced by the oxides are removed at the Te^0-$Pb_{1-x}Sn_xTe$ interface. If the mechanism of passivation could be established, one might hope to find even better surface

passivants than the Te^{O} discussed here. This could become crucial as devices with improved bulk leakage properties are produced or at temperatures below 77° K where bulk junction resistance increases rapidly.

ACKNOWLEDGMENTS

We thank E. R. Gertner and J. E. Clarke for materials preparation, and J. R. Waldrop for instrumentation design. We also thank M. D. Lind and E. H. Cirlin for X-ray analysis and SEM measurements. This work was supported by ONR Contract No. N00014-75-C-0344.

3.0 ADDITIONAL RESEARCH RESULTS

3.1 OBSERVATIONS OF Te° LAYERS ON SEMICONDUCTOR TELLURIDES

Elemental tellurium layers have been observed previously on CdTe after acid etching by Zitter[12] and by de Nobel[13]. In the course of our studies we have also observed these layers on SnTe, CdTe, and $Hg_{.8}Cd_{.2}Te$ in addition to the data on PbTe shown in the previous section. In Fig. 9 we show XPS spectra of Te° layers on SnTe and CdTe which were prepared by etching in HNO_3. Table IV tabulates some of our results on Te° layer thickness which were formed on the surfaces of these compounds. The layer thickness was determined by controlled A_r^+ ion sputtering as described in the previous section. Hall effect measurements were carried out on the SnTe sample which showed that it was p-type with a carrier concentration of $\sim 3 \times 10^{19}$ cm^{-3}. Thus, one interesting observation from the table is that Te° layers form on members of the $Pb_{1-x}Sn_xTe$ system of both carrier types. In another experiment Tl was diffused into a n-PbTe substrate to convert the surface to p-type. The Te° layer thickness formed on this surface compared to a surface which was not diffused shows that the thickness varied by more than an order of magnitude; this suggests that the Te° formation mechanism may depend on carrier type.

The surface morphology of Te° layers on n-PbTe and p-SnTe varies markedly as can be seen in the SEM micrographs shown in Fig. 10. It is not known yet if this morphlogy is correlated with carrier type, but in either case it is clear that the etchant (in this case HNO_3) has possible direct access to the substrate material and thus all results to date are consistent with a chemical mechanism for the Te° layer formation rather than some other mechanism (e.g., solid-state diffusion).

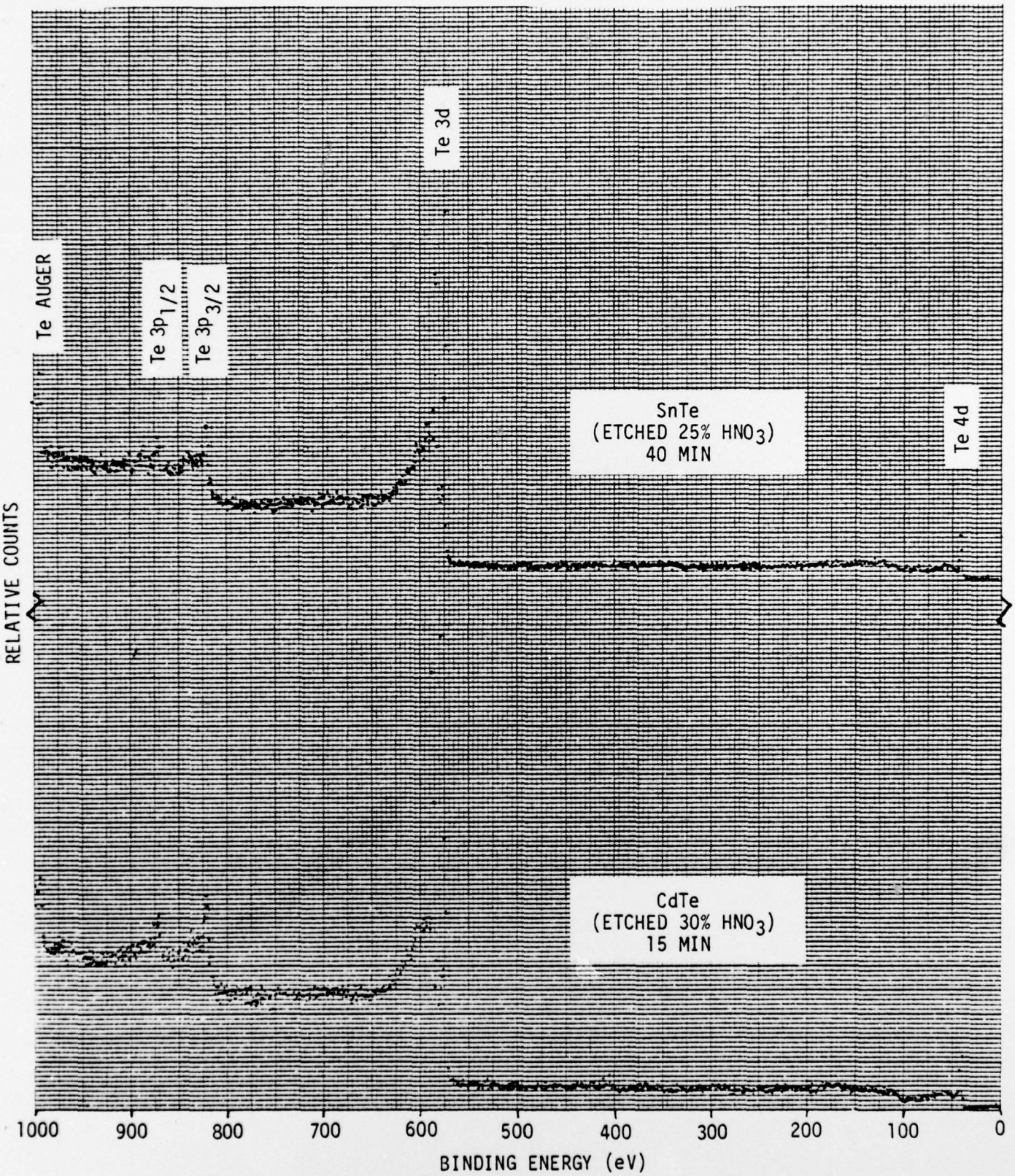

Figure 9. Te° layers observed on SnTe and CdTe.

Table IV. Te° layers observed on several tellurides.

Substrate	Etching Treatment	Te° Layer Thickness (Å)
p-SnTe ($\sim 3 \times 10^{19}$ cm^{-3})	25% HNO_3, 40 min, 25°C	400
p-SnTe ($\sim 3 \times 10^{19}$ cm^{-3})	25% HNO_3, 10 min, 25°C	240
CdTe	30% HNO_3, 15 min, 24°C	>7600
$Hg_{.8}Cd_{.2}Te$	30% HNO_3, 15 min, 24°C	<40
ZnTe	30% HNO_3, 15 min, 24°C	Te° did not form
n-PbTe ($\sim 10^{17}$ cm^{-3})	30% HNO_3, 15 min, 24°C	400
p-PbTe (Tl diffused)	30% HNO_3, 15 min, 24°C	>6000

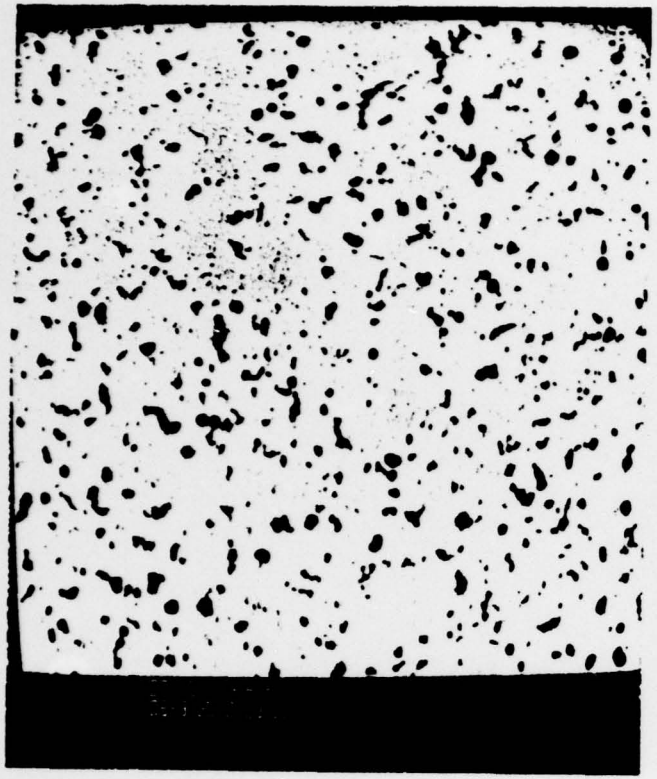

Te° layer on PbTe formed by etching with 25% HNO_3, 20 min., at 23°C.

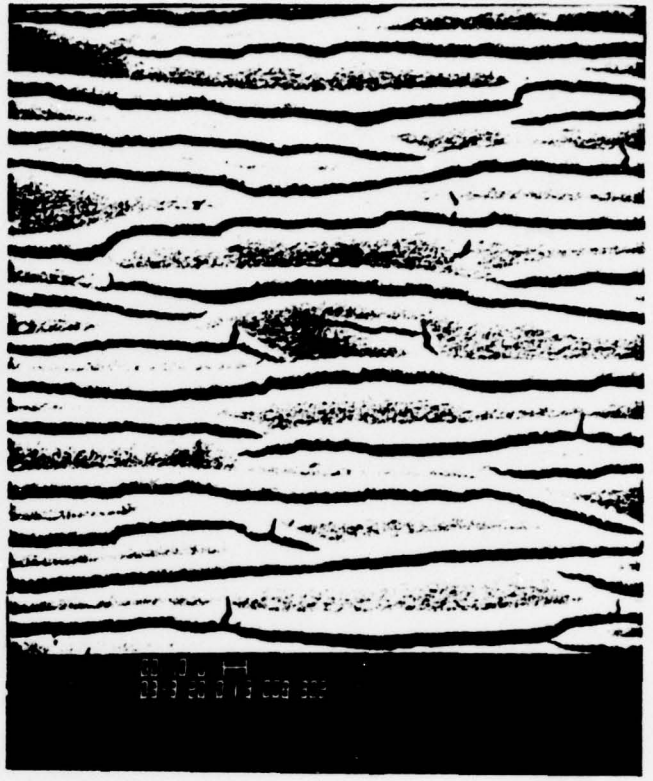

Te° layer on SnTe formed by etching with 25% HNO_3, 260 min., at 23°C.

Fig. 10 SEM Micrographs of Te° Layers on PbTe and SnTe (1 μm scale is indicated in photograph).

Previous studies of Te° layers on CdTe by using electron diffraction have established an amorphous nature of the Te° layers.[14] In one experiment we etched a sample of n-PbTe for 16 hours in 30% HNO_3 to build up a thick layer of Te°. Extrapolation of the data shown in Fig. 5 of the previous section on a log-log plot would predict a layer thickness of ≈ 5000Å. X-ray diffraction measurements carried out on a powder diffractometer failed to show any lines associated with crystalline Te - a result which we interpret as being consistent with an amorphous nature of the Te° layer.

The valence band density of states observed in XPS spectra has been shown[17] to be sensitive to the amphorous nature of Te in reasonable agreement with theoretical predictions.[18,19] In Fig. 11 we show valence band density of states of crystalline Te°, Te° formed on n-PbTe and Te° formed on p-SnTe. The marked difference in the valence band spectra of Te° on p-SnTe is obvious although the other 2 spectra are similar to within the accuracy of the data currently available (the data shown in the top of Fig. 9 and the data shown in the bottom of Fig. 11 were taken on the same surface). The nature of the amorphous form of Te is poorly known; most models assume atomic arrangements composed of broken chains, n-membered rings or some combination of both. The valence band density of states observed for Te° on SnTe certainly suggests a form of Te markedly different than trigonal Te°. It is not known at present whether or not this difference in valence band density of states correlates with the marked difference observed in surface morphology (Fig. 10).

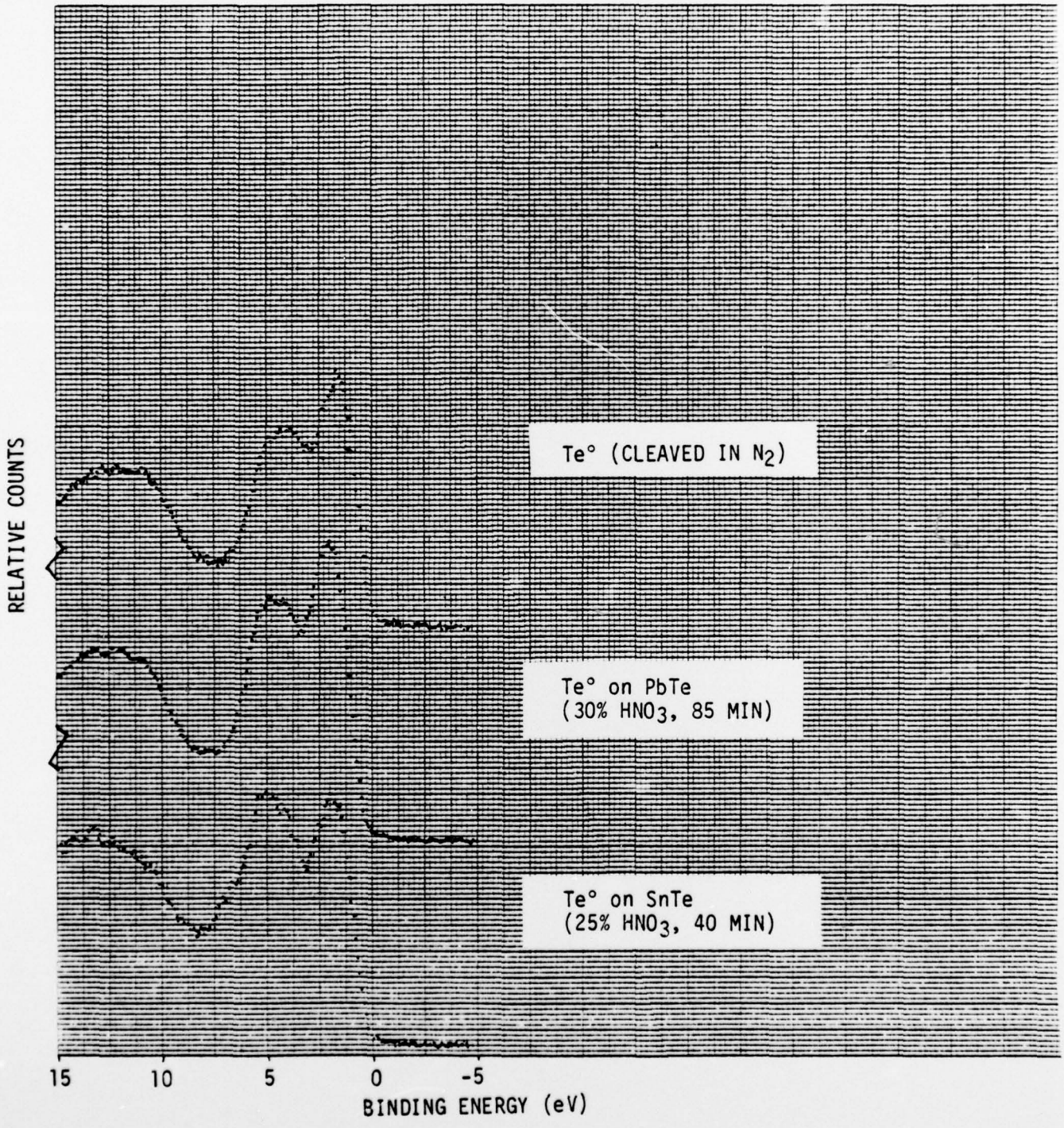

Figure 11. Valence band density of states for a) cleaved Te°, and Te° layers formed on b) PbTe and c) SnTe.

3.2 OXIDES ON $Pb_{1-x}Sn_xTe$ SURFACES

The nature of oxides found on $Pb_{1-x}Sn_xTe$ surfaces is known to strongly affect leakage characteristics of devices; thus we would like to be able to characterize these oxides. The approach used here is to compare XPS spectra of known oxide standards with oxides observed on $Pb_{1-x}Sn_xTe$ surfaces in order to identify oxidation states. This approach which was used to establish the oxidation state of Te as Te^{4+} was mentioned in the previous section. The approach relies on the ability to obtain XPS spectra of relatively clean well characterized standards. While this was possible for TeO_2, the study of Sn and Pb oxides proved to be very difficult. The main problem arose from fluorine contamination of the oxide surface which formed when samples were heated or sputtered in the high-vacuum system to remove normal surface contamination. The source of F is the teflon seals which are used on the standard Hewlett-Packard 5950A ESCA spectrometer. After exhausting most seemingly reasonable methods to overcome this problem, it was finally decided to completely replace the sample preparation chamber and inlet system with a high-vacuum, all metal seal modification. A photograph of this modification is shown in Fig. 12. The long bellows arrangement which replaces the standard teflon seals is clearly seen in the photograph. With this modification we are now able to heat and sputter insulating samples without introducing F contamination.

Although some data has been obtained on both Sn and Pb oxides, only the Sn oxide data has been analyzed in any detail as yet. Commercially available samples of SnO and SnO_2 were used for comparison with our data. The composition of these samples was checked with x-ray powder diffraction. Various heating and sputtering conditions were used to clean the samples.

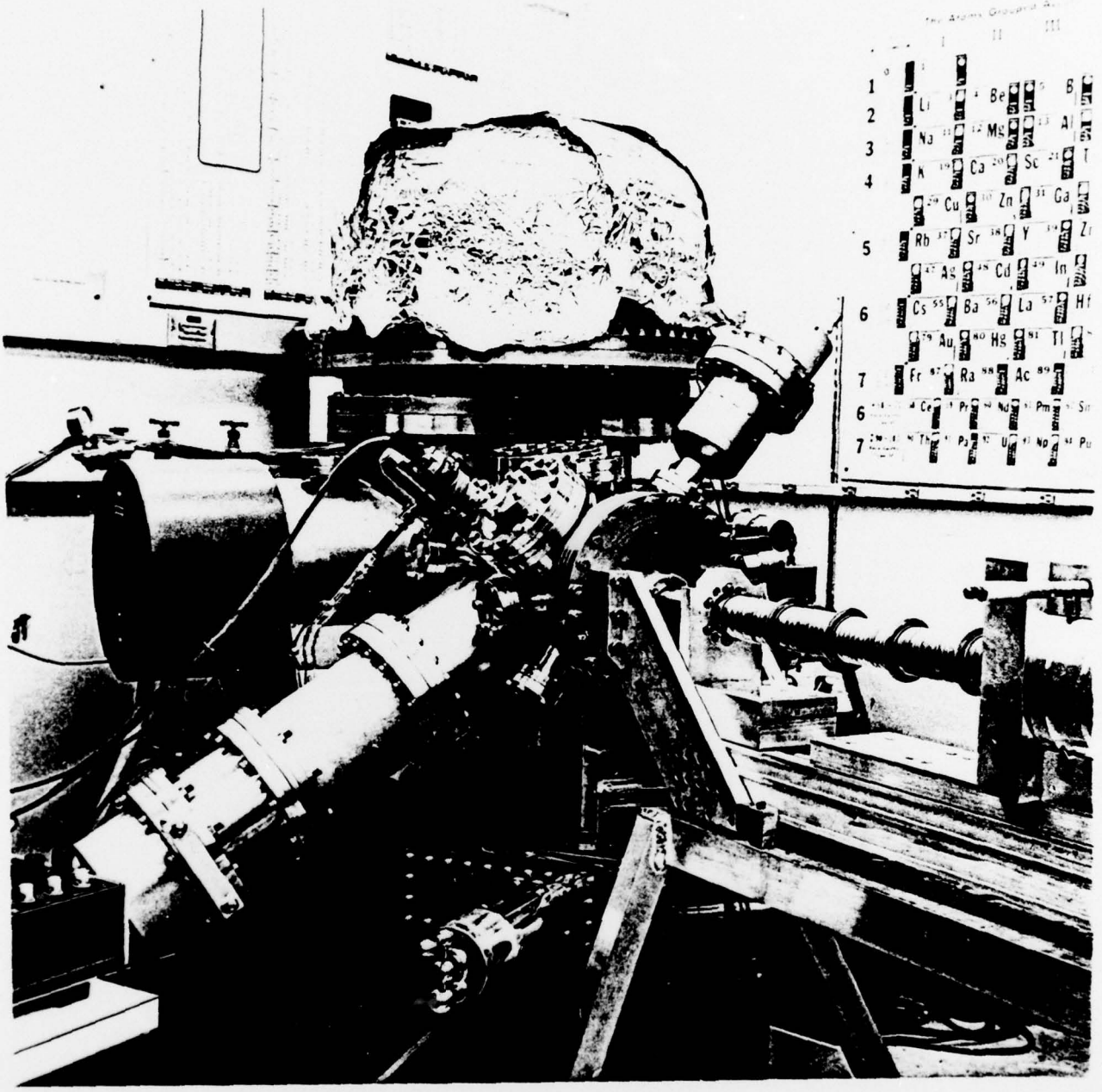

Fig. 12 All metal seal high-vacuum modification of Hewlett-Packard 5950A ESCA spectrometer. Photograph shows new sample preparation chamber and bellows system which replaces teflon seals.

The absence of photoelectron lines associated with elements other than Sn and O and the shape (width and symmetry) of the Sn and O core lines was used to assess sample purity. It was found that when "clean surfaces" of SnO and SnO_2 were obtained, their XPS spectra were identical (both line positions and relative line intensities).

It is possible to clean the surface of TeO_2 by heating the sample to $\approx$ 160°C. By using relative line intensity data for TeO_2 coupled with relative line intensity data in SnTe we estimate the relative cross-sections of the Sn $3d_{5/2}$/O $1s_{1/2}$ core levels to be $\approx$ 4.5. This ratio was used to establish that the outer surface observed on both SnO and SnO_2 was actually SnO; actual estimated values were $SnO_{.96}$ and $SnO_{.97}$. The alternative of assuming that the surface of Sn oxides was really SnO_2 would require that the surface of Te oxide have a composition of TeO_4 which seems unrealistic. The cause of the decomposition of the SnO_2 surface layer to SnO is not presently understood.

The Sn $3d_{5/2}$ and O $1s_{1/2}$ peak positions observed in SnO are 486.7 and 530.6, respectively, with an accuracy of $\pm$0.2 eV. To within experimental accuracy these binding energies correspond to binding energies observed for oxidized forms of Sn on $Pb_{1-x}Sn_xTe$ surfaces and thus we conclude that the most probable oxidation state of Sn on $Pb_{1-x}Sn_xTe$ surfaces is Sn^{2+}.

Several controlled oxidation studies of Sn, SnTe, Pb, and PbTe have been carried out. Although the data have not been fully interpreted, they show some striking results. In all cases the surfaces were cleaned in the XPS high vacuum chamber by A_r^+ sputtering and then exposed to O_2 in situ. The marked tendency for Sn to oxidize preferentially is dramatically demonstrated in Fig.13 for SnTe. In this figure XPS data in the

Figure 13. XPS spectra in region of Sn and Te $3d_{5/2}$ lines before and after exposure or SnTe to O_2.

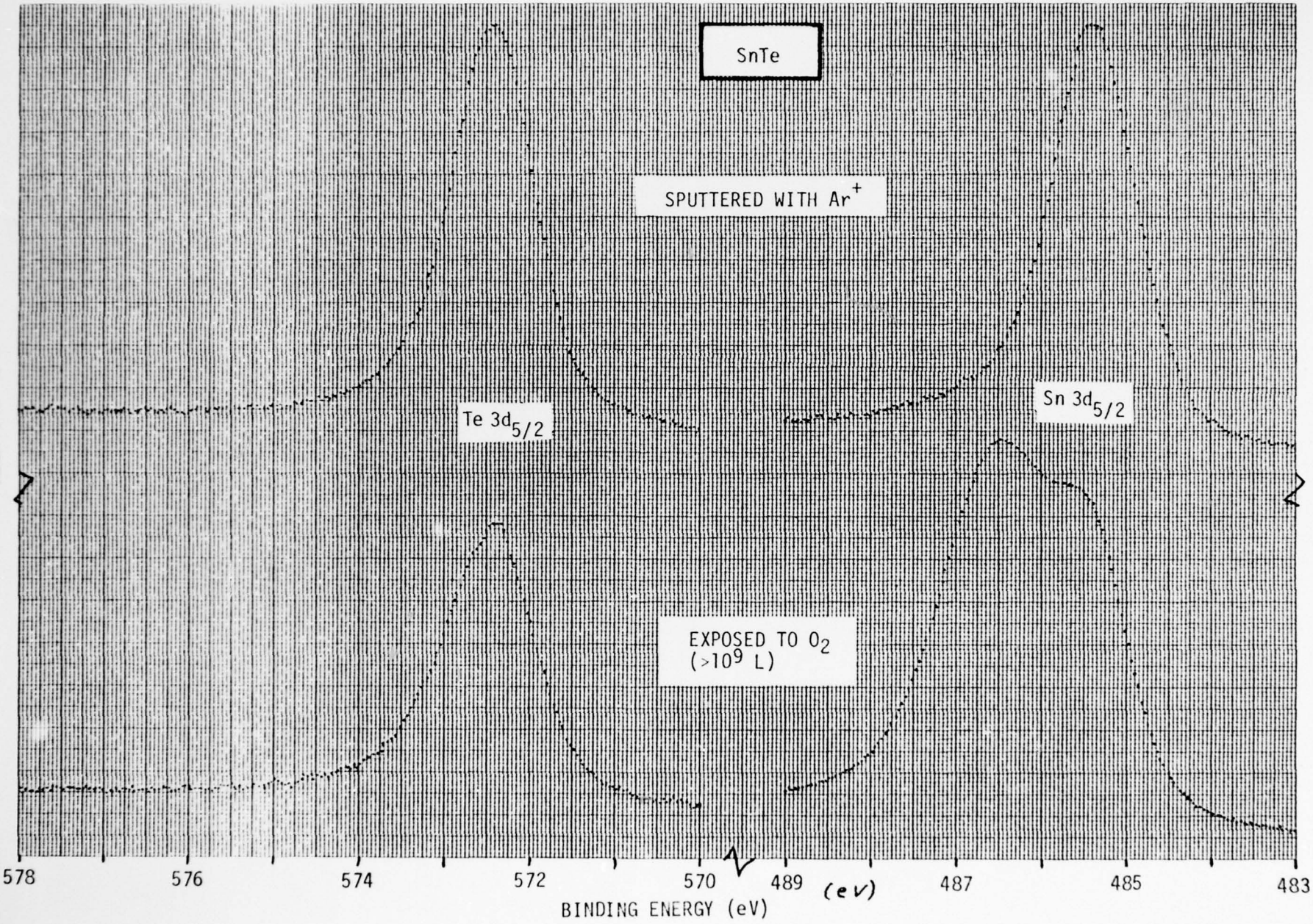

vicinity of the Sn $3d_{5/2}$ and Te $3d_{5/2}$ levels is shown. The analysis depth at the photoelectron kinetic energies being observed is 10-20Å. Figure 13 shows that at least several angstroms of Sn oxide are formed before the Te begins to oxidize. Similar preferential oxidation is not observed on PbTe.

3.3 SOME INITIAL XPS MEASUREMENTS ON $InAs_{1-x}Sb_x$

Until recently, epitaxial layers of $InAs_{1-x}Sb_x$ have not been available so that attempts to correlate device behavior with surface composition as described in Section 2 for $Pb_{1-x}Sn_xTe$ have not been possible. However, the effect of several surface treatments on the surface composition of $InAs_{1-x}Sb_x$ materials has been studied and large variations in surface stoichiometry have been observed. As an example in Fig. 14, we show XPS spectra in the regions of the As3d, Sb4d and In 4d levels. The data are for $InAs_{.87}Sb_{.13}$ which has been a) sputter cleaned, b) etched in HCl, and c) processed by several steps - the last one being a HNO_3 etch. The marked variations in surface stoichiometry is evident in the figure. It is interesting to note that in Fig. 14b a large excess of Sb is present while in Fig. 14c an As excess exists.

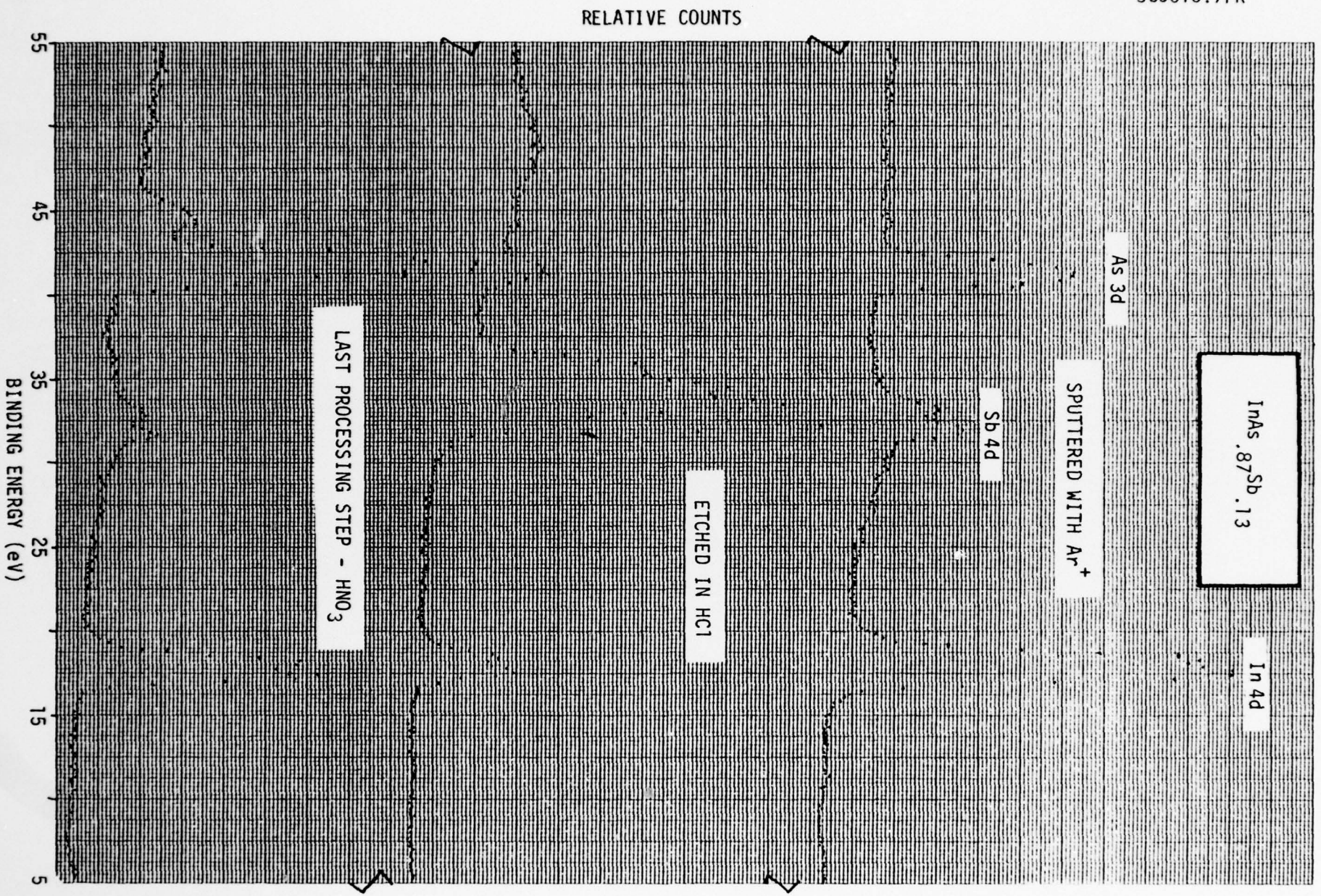

Figure 14. Large variations in surface stoichiometry resulting from processing $InAs_{.87}Sb_{.13}$.

4.0 REFERENCES

[1] J. W. Wagner and J. C. Woolley, Mat. Res. Bull. 2, 1055 (1967).

[2] N. R. Short, J. Phys. D 1, 129 (1968).

[3] J. T. Longo, E. R. Gertner, and A. S. Joseph, Appl. Phys. Lett. 19, 202 (1971)

[4] A. M. Andrews, J. T. Longo, E. R. Gertner, J. G. Pasko, J. E. Clarke, and P. Neuber, Proc. IRIS Detector Specialty Group Meeting, 1973.

[5] See e.g., C. R. Veale, J. Inorg. Nucl. Chem. 29, 1180 (1967).

[6] J. E. Coker, J. Electrochem. Soc. 116, 1021 (1969).

[7] R. Longshore, M. Jasper, B. Sumner, and P. LoVecchio, Infrared Physics 15, 311 (1975).

[8] P. C. Wang, M. H. Kalisher, J. M. Tracy and J. T. Longo, to be submitted for publication.

[9] H. Margenau and G. M. Murphy, "The Mathematics of Physics and Chemistry," Chapter 13, D. Van Nostrand Co., Inc., N.Y. Second Edition (1956).

[10] A. M. Andrews, "10.6 Micrometer PbSnTe Mosaic Development," Report No. AFAL-TR-74-111, 1974.

[11] M. K. Norr, J. Electrochem. Soc. 109, 433 (1962).

[12] R. N. Zitter, Surface Science 28, 335 (1971).

[13] D. de Nobel, U. S. Patent 2,822,299, Feb. 4, 1958. (This same author also has other patents related to this subject.)

[14] H. C. Montgomery, Solid State Electronics, 7, 147 (1964).

[15] R. N. Zitter and D. L. Chavda, J. Appl. Phys. 46, 1405 (1975).

[16] P. P. Debye, C. A. Kennedy, K. J. Linden, "Development of Lead-Tin Telluride Detectors," Contract No. DAAB09-69C-0045, B-002490, 1972.

[17]M. Schlüter, J. D. Joannupoulos, M. L. Cohen, L. Ley, S. P. Kowalczyk, R. A. Pollak and D. A. Shirley, Solid State Communications 15, 1007 (1974).

[18]M. Schlüter, J. D. Joannupoulos and M. L. Cohen, Phys. Rev. Lett. 33, 89 (1974).

[19]J. D. Joannopoulos, M. Schlüter and M. L. Cohen, Phys. Rev. B11, 2186 (1975).